

The laminar unsteady flow of a viscous fluid away from a plane stagnation point

By MARK J. HOMMEL†

Department of Mechanical Engineering, Stanford University

(Received 1 March 1982 and in revised form 15 March 1983)

The development with time of the impulsively started laminar flow of a viscous fluid away from a stagnation point is investigated. A series expansion in time is formulated for the shear stress and displacement thickness. This series expansion is obtained from a numerical solution of the full Navier–Stokes equations, and 44 terms are computed for the shear-stress series. The series is analysed and series-improvement techniques are employed to improve its convergence properties. The final series that results converges even for infinite time, and acceptable agreement with the Proudman & Johnson calculations of shear stress for steady-state flow at a stagnation point is obtained. Only 17 terms in the displacement-thickness series are reported, owing to numerical difficulties which are considerably more of an obstacle than in the shear-stress calculation. However, it is observed that the displacement thickness grows exponentially with time. Acceptable agreement with calculations of Proudman & Johnson is obtained for small time. For dimensionless time greater than 2.5, it is concluded that not enough terms are known to extrapolate the displacement-thickness series further.

1. Introduction

Proudman & Johnson (1962) have proposed an asymptotic expansion to model the time-dependent flow away from a stagnation point. This structure was studied in detail by Robins & Howarth (1972), who continued the asymptotic expansion. They found higher-order terms with an associated number of indeterminate constants which arose in the expansion. They also obtained a numerical solution of the full initial-value problem which supported their asymptotic expansion, at least for finite time values.

The line of reasoning of these papers is that, since the wake thickness grows very rapidly under the action of the convection field, the lengthscale normal to the flow boundary becomes much larger than the distance over which viscous forces are important. It was therefore conjectured that the viscous term in the governing equation is important only near the boundary, and a major portion of the flow region for large times is governed by the inviscid equation. A similarity solution of the inviscid equation was obtained which showed that the boundary-layer thickness increases exponentially with time. It follows from this solution that the flow in a local region away from a stagnation point ultimately becomes steady flow towards a stagnation point, even as the global size of the reverse-flow region continues to grow. The global skin friction at the stagnation point would therefore tend to a finite negative value, equal in magnitude and opposite in sign to that of flow towards a stagnation point.

† Present address: F. G. Bercha and Associates, Houston, Texas.

In the present study, we attempt to model once again the laminar flow of an incompressible fluid with small viscosity away from a stagnation point. This is an idealized local solution at a point for all time. The approach taken is to formulate a series expansion in time for the shear stress at the stagnation point, and then to apply series-improvement techniques with the hope of extrapolating to large times. It is well known that transformations can improve the accuracy of a power series as well as extend its radius of convergence. Such an approach has proven successful in other problems (see e.g. Van Dyke 1970) where the series was found to be limited by a radius of convergence lacking physical meaning. This radius of convergence is defined by the series' pole nearest to the origin in the complex plane. For poles not on the positive real axis for a physical variable, no physical meaning can be attached to the pole. The series could then be improved by analytic continuation into the region outside the radius of convergence, for physically interesting values of the expansion variable. If only a finite number of terms for the series is known, and the radius of convergence can be estimated, a practical method of analytical continuation is to banish the offending pole (or, more generally, singularity) to infinity with a linear fractional transformation, such as an Euler transformation. This is achieved by introducing the transformation and recasting the series in powers of the new variable. In terms of the new variable, the series is then not unnecessarily restricted from converging. This approach is appealing because it does not rely on a numerical model of the entire two-dimensional flow field, but rather appeals to the principles of analytical continuation for a power series.

2. Method of solution

Dimensional coordinates x' and y' are defined tangential and normal to the flow boundary respectively, with x' measured away from the stagnation point. We define non-dimensional coordinates as follows:

$$x = \frac{x'}{a}, \quad y = y' \left(\frac{2U_0}{\nu a} \right)^{\frac{1}{2}}, \quad t = \frac{2U_0 t'}{a}, \quad (2.1)$$

where U_0 is the speed of the stream at infinity, a is a characteristic length, ν is the kinematic viscosity and t' is the time. In a small region near the stagnation point, the potential flow corresponding to an impulsive start is described by the stream function,

$$\psi' = -(2\nu a U_0)^{\frac{1}{2}} xy. \quad (2.2)$$

Following Proudman & Johnson (1962), this potential solution is enforced as the outer boundary condition for all time. Then the Navier–Stokes equations are solved exactly by setting

$$\psi' = -(2\nu a U_0)^{\frac{1}{2}} xF(y, t) \quad (2.3)$$

to obtain the following differential equation with initial and boundary conditions:

$$\left. \begin{aligned} F_{yt} - F_{yyy} &= (-1 + F_y^2 - FF_{yy}), \\ F(0, t) = F_y(0, t) &= 0, \\ F_y(\infty, t) &= 1, \\ F_y(y, 0) &= 1 \quad (y \neq 0). \end{aligned} \right\} \quad (2.4)$$

At this point the present analysis departs from that of Proudman & Johnson. A solution to (2.4) is sought as an expansion in time from $t = 0$, rather than assuming

1	1.1283791671	23	-0.1976×10^{-10}
2	-1.60727816	24	-0.9133×10^{-11}
3	-0.2480917	25	-0.1530×10^{-12}
4	0.14290×10^{-1}	26	0.8296×10^{-12}
5	0.28692×10^{-1}	27	0.1985×10^{-13}
6	0.63774×10^{-2}	28	-0.3284×10^{-13}
7	-0.15147×10^{-2}	29	-0.2569×10^{-13}
8	-0.10750×10^{-2}	30	-0.2811×10^{-14}
9	-0.97361×10^{-4}	31	0.1717×10^{-14}
10	0.89268×10^{-4}	32	0.6626×10^{-15}
11	0.30662×10^{-4}	33	-0.262×10^{-17}
12	-0.18844×10^{-5}	34	-0.6351×10^{-16}
13	-0.34650×10^{-5}	35	-0.1522×10^{-16}
14	-0.61583×10^{-6}	36	0.2526×10^{-17}
15	0.19425×10^{-6}	37	0.2129×10^{-17}
16	0.10522×10^{-6}	38	0.2511×10^{-18}
17	0.58123×10^{-8}	39	-0.1575×10^{-18}
18	-0.8889×10^{-8}	40	-0.6075×10^{-19}
19	-0.26564×10^{-8}	41	0.2687×10^{-20}
20	0.24906×10^{-9}	42	0.6591×10^{-20}
21	0.3176×10^{-9}	43	0.1050×10^{-20}
22	0.4865×10^{-10}	44	-0.4285×10^{-21}

TABLE 1. Values of $f_n''(0)$ for rear stagnation point

an asymptotic form of the flow a long time after the start. Seeking such a solution to the full Navier–Stokes equations obviates the necessity of using a matched asymptotic expansion. Equation (2.4) is uniformly valid.

The expansion which is formed conveniently treats initial viscous-diffusion effects and also properly handles the boundary conditions. We set

$$F = 2t^{\frac{1}{2}}\{f_1(\eta) + tf_2(\eta) + t^2f_3(\eta) + \dots\}, \quad (2.5)$$

where $\eta = y/2t^{\frac{1}{2}}$. Substituting this expansion into the full problem (2.4) gives a series of linear, third order, ordinary differential equations similar to those solved by Collins & Dennis (1973). The equations are solved by employing the finite-difference scheme of Collins & Dennis. This scheme is $O(h^6)$ and is exceedingly accurate.

The main result sought here is the shear stress at the boundary given by

$$\tau'_{xy} = \rho\nu^{\frac{1}{2}}\left(\frac{U_0}{a}\right)^{\frac{3}{2}}x' \frac{1}{2t^{\frac{1}{2}}} \sum_{n=1}^{\infty} f_n''(0)t^{n-1}, \quad (2.6)$$

where τ'_{xy} is the dimensional shear stress at the flow boundary and ρ is the fluid density.

A total of 44 terms was obtained using an IBM 370/168. These terms are tabulated in table 1. The terms in (2.6) were obtained using extended precision, which carries 35 significant figures, and then comparing with double precision, which carries 16 significant figures, to monitor round-off error. The accuracy of the numerical scheme was evaluated by comparing the computed values of $f_2''(0)$ and $f_3''(0)$ with their exact values, given by Wundt's (1955) boundary-layer solution. This is possible because the full Navier–Stokes equation applied at a plane wall degenerates to equations identical with the boundary-layer equations solved by Wundt. No comparison was performed for $f_1''(0)$ because f_1 was obtained by integrating the exponential function

twice. Comparison was also made with the numerical results of Collins & Dennis (1973) for the first eight $f_n''(0)$ and agreement is excellent. Details are available in Hommel (1981).

As the calculation using a mesh size $h = 0.01$ came the closest to reproducing the exact values of $f_2''(0)$ and $f_3''(0)$, the somewhat conservative approach was adopted of reporting as significant figures only as many digits to which the $h = 0.01$ and $h = 0.025$ calculations agree. The boundary condition at infinity was actually imposed at $\eta = 5$ and then checked with another solution using $\eta = 12.5$. No significant difference in the shear stress at $\eta = 0$ was observed. Having thus established the accuracy of the numerical method, the 44 terms calculated for (2.6) are given in table 1.

3. Series analysis

The analysis procedure to follow is motivated by considering the model function

$$f(\epsilon) = (1 + \epsilon)^{-1} = 1 - \epsilon + \epsilon^2 - \epsilon^3 + \dots, \tag{3.1}$$

which has a singularity at $\epsilon = -1$, and hence a radius of convergence of 1. We introduce an Euler transformation

$$\delta = \frac{\epsilon}{1 + \epsilon}. \tag{3.2}$$

It is found that the new series terminates after only two terms:

$$f(\delta) = 1 - \delta. \tag{3.3}$$

The new series (3.3) represents the original series (3.1) throughout the δ -plane. Its advantage is that the singularity present at $\epsilon = -1$ in (3.1) has been mapped to $\delta = \infty$ in (3.3). The techniques presented here represent a generalization of this approach.

In figure 1 the Cauchy Root Test is used to estimate the radius of convergence of the series (2.6). A radius of convergence of approximately 3 is indicated.

Next, we consider the sign pattern in table 1 to obtain further information about the location of the nearest singularity. For coefficients numbered 4, ..., 44, the sign pattern is (+ + + - - - + + - - - + + + - -) with the exceptions of coefficients numbers 33 and 41. Note, however, that both the 33rd coefficient and the 41st coefficient are smaller than would be expected from examining their neighbours.

As pointed out by Van Dyke (1980), a sign pattern is associated with a complex-conjugate pair of singularities forming angles β and $-\beta$ with the real axis in the complex plane. That is, the sum of two simple poles gives the model function

$$\frac{1}{2} \left\{ \frac{1}{e^{i\beta} - z} + \frac{1}{e^{-i\beta} - z} \right\} = \sum_{n=0}^{\infty} z^n \cos(n + 1)\beta. \tag{3.4}$$

The period of the sign pattern mentioned above is 16, and so a value of $\beta = \frac{1}{16}\pi m$ in (3.4) reproduces the sign pattern displayed for coefficients 4, ..., 44. Calculation of sign patterns for various values of m and comparison with table 1 implies $m = 6$, locating the nearest singularities on the rays $\pm 67.5^\circ$. The value of β obtained by this analysis, however, is not necessarily unique, even though a unique value of β is associated with any given sign pattern. Fortunately, the final calculated value of the shear stress is not strongly dependent on the value of β chosen. More will be said of this later.

Additional information can be obtained from the Padé approximants $P(M/N)$. A Padé approximant is a rational fraction with numerator of degree M and denominator

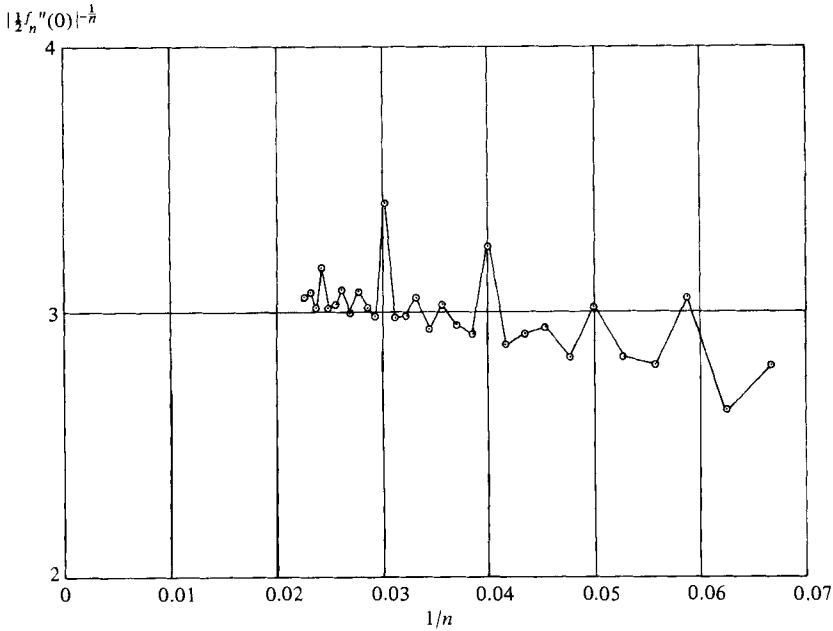


FIGURE 1. Cauchy Root Test for shear stress.

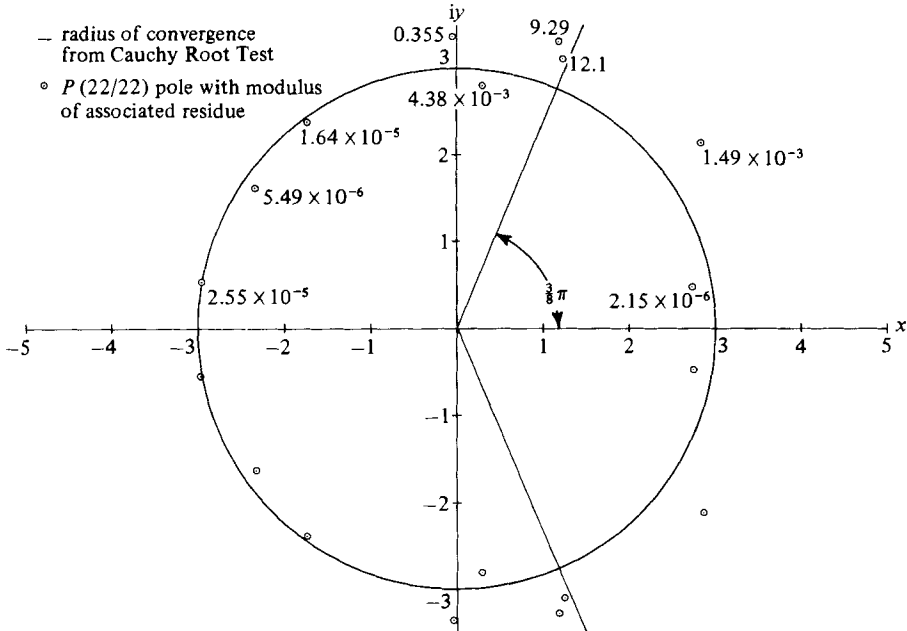


FIGURE 2. Location of poles for stagnation point from Padé analysis.

of degree N that reproduces a given power series to $M+N+1$ terms when the Padé approximant is expanded. The poles of a Padé approximant are related to the singularities whose existence is suggested by the sign pattern of table 1. We expect that taking successively more terms in the Padé approximant will provide increasingly refined estimates of the location of the nearest complex singularity. Figure 2 shows the complex plane and the location of the poles as suggested by the sign pattern as

well as the location calculated by means of the Padé approximants. It appears that the singularity at $\beta = \frac{2}{3}\pi$ dominates the sign pattern and hence the series itself. Indeed, the residues of the associated singularities obtained in the Padé analysis are at least several orders of magnitude larger than the residues of any other singularity, even those which are somewhat closer to the origin. For example, the residue magnitudes given by $P(22/22)$ are 12.1, 9.29 and 0.355 for poles at angles 67.9° , 70.5° and 90.5° respectively. All other residue magnitudes are less than 0.005. Closer examination reveals that the Padé approximants' estimates of the singularity's location remains consistent with increasing N . Under-flow limitations of the computer prevented calculation of Padé approximants $P(N/N)$ of order $N > 22$, using further terms of (2.6) which are reported by Hommel (1981). Nevertheless, the Padé approximants do increase our confidence in having established the location of the nearest singularity.

The Padé analysis further shows that the first zero of the rear stagnation-point shear stress is at $t = 0.643839707$. This number provides yet another check on the accuracy of the analysis because the time at which the shear stress goes to zero is a widely published number which has been calculated in a variety of ways. The following comparisons include the result of just three past studies:

present study (dividing by 2 for same coordinates)	0.32191985	(44 terms)
Collins & Dennis (1973)	0.3220	(7 terms)
Goldstein & Rosenhead (1936)	0.3195	(3 terms)
Blasius (1908)	0.35	(2 terms)

Agreement is satisfactory.

We now attempt to improve the convergence properties of the series in order to extrapolate the solution to larger times. To do this we employ a complex transformation analogous to the real Euler transformation (3.2). The dominant singularity is banished to infinity by setting

$$u = \frac{Rt}{(t^2 - 2tR \cos \beta + R^2)^{\frac{1}{2}}}, \quad (3.5)$$

where the dominant singularity pair is located at a radius of R from the origin and at angles of $\pm\beta$ in the complex t -plane. As pointed out by Pearce (1978), this transformation may be considered to be a generalization of the Euler transformation given in (3.2). The value of R is suggested to be 3 from the Cauchy Root Test. We choose $\beta = 67.5^\circ$, in accordance with the sign pattern in table 1, acknowledging that the final results are not sensitive to the exact values of R and β chosen. This will be discussed later.

We recast (2.6) using (3.5) to obtain

$$\frac{\tau'}{\rho^{1/2} U_1^3 x'} = \frac{1}{u^3} \sum_{n=1}^{44} d_n u^{n-1}, \quad (3.6)$$

where $U_1 = U_0/a$. Values for the d_n coefficients are given by Hommel (1981). The coefficients alternate in sign after the 19th term, suggesting the nearest singularity for (3.6) is now on the negative real axis.

Examination of the inverse transformation of (3.5) shows that the generalized Euler transformation introduces spurious singularities which are not present in the original

t	$\frac{\tau'}{\rho\nu^{\frac{1}{2}}U_1^{\frac{3}{2}}x'}$	Numerical solution (Howarth 1981 personal communication to M. Van Dyke)
0.5	0.188418298	0.18821
1.0	-0.340102048	-0.34009
1.5	-0.666419214	-0.66647
2.0	-0.88421920	-0.88437
2.5	-1.02239	-1.0226
3.0	-1.10479	-1.1051
3.5	-1.1524	-1.1528
4.0	-1.180	-1.1808
4.5	-1.197	-1.1981
5.0	-1.210	-1.2094
5.5	-1.220	-1.2170
6.0	-1.22	—
6.5	-1.23	—
7.0	-1.23	—
7.5	-1.23	—

TABLE 2. Computed values for the shear stress

series. The inverse of (3.5) is

$$t = \frac{Ru^2 \cos \beta - R^2u(1 - (u \sin \beta/R)^2)^{\frac{1}{2}}}{u^2 - R^2}. \tag{3.7}$$

In our case, $\beta = 67.5^\circ$, and hence $0 < \beta < \frac{1}{2}\pi$. Pearce (1978) has shown that, for such a value of β , the inverse transformation has a pole at $u = -R$ and a branch point at $u = R/\sin \beta$.

Following Pearce (3.5), an Euler transformation is now introduced with $R = 3$ in

$$\xi = \frac{Ru}{u + R} \tag{3.8}$$

to obtain

$$\frac{\tau'}{\rho\nu^{\frac{1}{2}}U_1^{\frac{3}{2}}x'} = \frac{1}{\xi^{\frac{3}{2}}} \sum_{n=1}^{44} c_n \xi^{n-1}. \tag{3.9}$$

Values for the c_n coefficients are given by Hommel (1981). Summing the series for values of t produces the results presented in table 2. Note that Howarth's (1981 personal communication to M. Van Dyke) solution is obtained from a numerical integration of the full Navier-Stokes equations as applied to a plane boundary. Setting $\xi = \frac{1}{2}R$ corresponding to $u = R, t \rightarrow \infty$ in (3.9) gives

$$\tau' = -1.23\rho\nu^{\frac{1}{2}}U_1^{\frac{3}{2}}x', \tag{3.10}$$

which supports the value of -1.23259 , suggested by the model of Proudman & Johnson.

The accuracy of the values of R and β , of course, is somewhat questionable owing to how they were found: R by graphical extrapolation; β by analogy with a model function. While the model function is unique for a given sign pattern, the sign pattern itself is not necessarily unique, being dependent upon the analyst's judgement. It is

n	(3.11)	(3.12)	(3.13)	(3.14)
1	0.5641895835	0.5641895835	0.5641895835	0.5641895835
2	0.41984	-0.14435	-0.16068	-0.66646 $\times 10^{-1}$
3	0.2448	0.1070	0.1355	0.7866 $\times 10^{-1}$
4	0.8423 $\times 10^{-1}$	-0.4468 $\times 10^{-1}$	-0.7410 $\times 10^{-1}$	0.1187 $\times 10^{-1}$
5	0.470 $\times 10^{-2}$	-0.360 $\times 10^{-2}$	0.243 $\times 10^{-1}$	-0.738 $\times 10^{-2}$
6	-0.1157 $\times 10^{-1}$	-0.2163 $\times 10^{-2}$	-0.1530 $\times 10^{-1}$	-0.1504 $\times 10^{-1}$
7	-0.5804 $\times 10^{-2}$	0.1562 $\times 10^{-2}$	0.6004 $\times 10^{-2}$	-0.1475 $\times 10^{-1}$
8	-0.403 $\times 10^{-3}$	0.773 $\times 10^{-3}$	-0.252 $\times 10^{-2}$	-0.112 $\times 10^{-1}$
9	0.897 $\times 10^{-3}$	0.909 $\times 10^{-4}$	0.122 $\times 10^{-2}$	-0.726 $\times 10^{-2}$
10	0.47 $\times 10^{-3}$	-0.10 $\times 10^{-3}$	-0.46 $\times 10^{-3}$	-0.40 $\times 10^{-2}$
11	0.47 $\times 10^{-4}$	-0.58 $\times 10^{-4}$	0.21 $\times 10^{-3}$	-0.18 $\times 10^{-2}$
12	-0.62 $\times 10^{-4}$	-0.74 $\times 10^{-5}$	-0.87 $\times 10^{-4}$	-0.46 $\times 10^{-3}$
13	-0.35 $\times 10^{-4}$	0.71 $\times 10^{-5}$	0.35 $\times 10^{-4}$	0.17 $\times 10^{-3}$
14	-0.41 $\times 10^{-5}$	0.45 $\times 10^{-5}$	-0.15 $\times 10^{-4}$	0.38 $\times 10^{-3}$
15	0.42 $\times 10^{-5}$	0.39 $\times 10^{-6}$	0.59 $\times 10^{-5}$	0.39 $\times 10^{-3}$
16	0.25 $\times 10^{-5}$	-0.41 $\times 10^{-6}$	-0.22 $\times 10^{-5}$	0.30 $\times 10^{-3}$
17	0.3 $\times 10^{-6}$	-0.4 $\times 10^{-6}$	0.6 $\times 10^{-6}$	0.2 $\times 10^{-3}$

TABLE 3. Displacement-thickness series coefficients

gratifying therefore that varying R from 3.0 to 3.4 causes no changes in values of the shear stress calculated from (3.9) for finite values of time, to the number of significant figures shown in table 2. Changing β from 67.5° , which corresponds to the sign pattern of table 1, to 80° , also produced no change. Varying R in the second transformation from 1.5 to 3.0 likewise produced no change in computed values of the shear stress.

An attempt was also made to calculate displacement thickness. The calculation of displacement thickness is much more difficult than the calculation of the wall shear stress. This is due to the exponential decay of the flow properties at infinity. The accuracy of the calculation of $f_n(\infty)$ is more susceptible to truncation and round-off errors as well as errors caused by locating the outer boundary condition at some finite value of η instead of at 'infinity'. Of the three sources of error, round-off error most quickly swamps the accuracy of the calculation, and it was concluded that only 17 terms in the series expansion for displacement thickness could be reported.

The displacement thickness is given by

$$\delta'_1 = \left(\frac{av}{U_0}\right)^{\frac{1}{2}} 2t^{\frac{1}{2}} \sum_{n=1}^{17} b_n t^{n-1}. \quad (3.11)$$

Values of the b_n coefficients are given in table 3.

We now extract a factor e^t from the series (3.11) in anticipation of the form of the solution given by Proudman & Johnson:

$$\left(\frac{U_0}{av}\right)^{\frac{1}{2}} e^{-t} \delta'_1 = 2t^{\frac{1}{2}} \sum_{n=1}^{17} a_n t^{n-1}. \quad (3.12)$$

Values for the a_n coefficients are given in table 3. We then assume the same location for the nearest singularity as was obtained for the shear stress, and introduce (3.5) into (3.12) to obtain

$$\left(\frac{U_0}{av}\right)^{\frac{1}{2}} e^{-t} \delta'_1 = 2u^{\frac{1}{2}} \sum_{n=1}^{17} d_n u^{n-1}, \quad (3.13)$$

t	$\left(\frac{U_0}{\nu a}\right)^{\frac{1}{2}} \delta_1$ (equation (3.14))	$\left(\frac{U_0}{\nu a}\right)^{\frac{1}{2}} \delta_1$ (Numerical solution, Howarth (1981 personal communication to M. Van Dyke))
0.5	1.195974	1.1961
1.0	2.6026	2.6067
1.5	4.719	4.7385
2.0	7.5	7.5938
2.5	11.0	11.246
3.0	15.0	16.231
3.5	20.0	23.708
4.0	—	35.614
4.5	—	55.129
5.0	—	87.558
5.5	—	141.860

TABLE 4. Displacement thickness as a function of time

whose coefficients are tabulated in table 3. The signs of the series alternate, as was expected. The transformation (3.8) is then introduced to obtain

$$\left(\frac{U_0}{\nu a}\right)^{\frac{1}{2}} e^{-t} \delta_1' = \xi^{\frac{1}{2}} \sum_{n=1}^{17} c_n \xi^{n-1}. \quad (3.14)$$

The c_n coefficients are listed in table 3. It is not possible to exploit a sign pattern here because not enough terms are available upon which to base conclusions. Calculated values for the displacement thickness as a function of time are presented in table 4. The unimpressive showing of series improvement techniques here is due to not having enough terms to work with. Unfortunately, computer round-off limitations prohibited our obtaining more terms in the series, and this phase of the study was halted.

4. Conclusions

Whereas Robins & Howarth (1972) had to integrate the equations out to $\eta = 500$, the present study's series-improvement technique for the shear-stress series only required an integration out to $\eta = 5$. All of the information required to examine the flow for all time is contained in the initial-value problem for small time. We have obtained 44 terms in the time series for the shear stress and have succeeded in calculating values for the shear stress for all time, even $t \rightarrow \infty$. Using this technique, we have verified Proudman & Johnson's (1962) prediction that the shear stress for flow away from a stagnation point is equal in magnitude and opposite in sign to the shear stress for flow toward a stagnation point. This was achieved without making any prior assumption regarding the nature of the steady-state flow. The flow reverses itself at approximately $t = 0.64$. This reverse flow occurs abruptly at $t = 0.64$ for all x and the region grows thereafter exponentially with time. It has recently been brought to my attention that this problem has also been investigated by Cowley (1981), who has found 43 terms of the associated series expansion, using a slightly different approach.

I am grateful to Professor Milton Van Dyke for many stimulating discussions regarding this problem, and also for suggesting it in the first place. I would like to express my appreciation to my former employer, Marathon Oil Company, for providing an environment in which higher education is encouraged.

REFERENCES

- BLASIUS, H. 1908 Grenzsichten in Flüssigkeiten mit kleiner Reibung. *Z. Math. Phys.* **56**, 1.
- COLLINS, W. M. & DENNIS, S. C. R. 1973 The initial flow past an impulsively started circular cylinder. *Q. J. Mech. Appl. Maths* **26**, 53.
- COWLEY, S. J. 1981 Unsteady separation. *Presented at EUROMECH 148, 13–15 Oct., Ruhr University, Bochum, Germany.*
- GOLDSTEIN, S. & ROSENHEAD, L. 1936 Boundary layer growth. *Proc. Camb. Phil. Soc.* **32**, 392.
- HOMMEL, M. J. 1981 Ph.D. dissertation, Stanford University.
- PEARCE, C. J. 1978 *Adv. Phys.* **27**, 89.
- PROUDMAN, I. & JOHNSON, K. 1962 Boundary layer growth near a rear stagnation point. *J. Fluid Mech.* **12**, 161.
- ROBINS, A. J. & HOWARTH, J. A. 1972 Boundary layer development at a two-dimensional rear stagnation point. *J. Fluid Mech.* **56**, 161.
- VAN DYKE, M. 1970 Extension of Goldstein's series for the Oseen drag of a sphere. *J. Fluid Mech.* **44**, 365.
- VAN DYKE, M. 1980 Notes on computer-extended series in mechanics. *Prepared for the 20th Summer Res. Inst. of the Austral. Math. Soc., Canberra, 14 Jan.–8 Feb. 1980.*
- WUNDT, H. 1955 Wachstum der laminaren Grenzschicht an schräg angeströmten Zylindern bei Anfahrt aus der Ruhe. *Ing.-Arch.* **23**, 212.